電気学会論文誌 C（電子・情報・システム部門誌）
IEEJ Transactions on Electronics, Information and Systems
Vol.131 No.9 pp.1528-1534 DOI: 10.1541/ieejeiss.131.1528

Paper

Ultrasound Phantom Using Thin Wires for the Depiction of Calcification

— Comparison of Cross-Sections of Wire Targets and Mass Targets —

Hirofumi Taki* Member, Takuya Sakamoto* Member
Makoto Yamakawa** Member, Tsuyoshi Shiina*** Member
Toru Sato* Member

(Manuscript received Jan. 20, 2011, revised June 7, 2011)

We report on a technique to construct an ultrasound calcification phantom using wires. Employment of the proper angle of the measurement plane to a wire target can adjust its effective size to that of a mass target. To acquire this angle of the measurement plane we compared the scattering cross-sections of 0.2, 0.1, 0.05 and 0.03 mm diameter copper wires, and copper cylinders that are 0.2 and 0.1 mm in size. The experiments were conducted using a commercial ultrasonographic device with a 7.5 MHz linear array probe. The scattering cross-section of a wire is severely reduced as the angle of the measurement plane to that wire decreases. At a depth of 2 cm the scattering cross-sections of the 0.2 and 0.1 mm copper cylinders are equivalent to the scattering cross-section of a 0.1 mm diameter copper wire, when the measurement plane angles to the wire are 87.6 and 87.0 degrees for the 0.2 and 0.1 mm copper cylinders, respectively. This result indicated that the employment of the proper angle of the measurement plane can adjust the effective size of a wire target to the size of a mass target, and consequently fulfills the requirements for use as a calcification phantom.

Keywords : ultrasonography, calcification, scattering cross-section, effective size, ultrasound phantom

1. Introduction

Ultrasonography (US) provides a great deal of information about soft tissue that is important for the diagnoses of various diseases. However, US has a limited ability to detect calcifications compared with X-ray imaging such as X-ray computed tomography and mammography[(1)-(4)]. The existence of calcifications not only causes pain and various diseases but also indicates the presence of lethal diseases. Renal calcification causes acute pain, kidney infection and hydronephrosis. Gallstones are intensely painful. The existence of diffuse calcifications in the breast indicates breast cancer. Because US is a convenient, safe and effective clinical imaging tool involving no exposure to ionizing radiation, improvement in its calcification detection ability is desirable.

Many researchers have proposed medical ultrasound imaging techniques to improve the spatial resolution of US. Tissue harmonic imaging (THI) is one of the techniques that have been used to improve the spatial resolution of US. THI suppresses speckle artifacts and improves contrast resolution[(5)-(7)]; however, the calcification detection ability of THI is considerably lower than that of X-ray imaging. Other researchers have employed a cell-averaging constant false alarm rate (CA CFAR) to depict calcification[(8)(9)]. The CA CFAR extracts targets from non-stationary noise and clutter while maintaining a constant probability of a false alarm[(10)(11)]. Therefore, CA CFAR detectors can depict calcifications with high-intensity echoes but can rarely detect small calcifications. This is due to the fact that they have inconspicuous echo intensities as compared with the surrounding tissue.

To enable the depiction of calcifications without high-intensity echoes, we have proposed a calcification depiction method for US using decorrelation of echoes (CDDE) caused by calcifications[(12)-(14)]. Since CDDE inspects the waveform change caused by a calcification, it can depict a wire of diameter 0.05 mm that is only faintly depicted in a B-mode image due to its slight echo intensity[(15)]. CDDE also results in clear depiction of a calcification that is faintly depicted in a B-mode image; however, the employment of a small mass target to mimic a calcification results in difficulty in confirming that the mass target is located in the measurement plane. Therefore, we have previously investigated the performance of CDDE for ultrasonography in the depiction of calcification using wire targets. Because a calcification is a kind of mass target, the evaluation of the performance of CDDE requires that the effective size of the wire targets and mass targets be similar. Since the angle of the measurement plane to a wire is supposed to strongly influence the scattering cross-section of a wire target, the employment of the proper angle of the measurement plane is expected to adjust the scattering cross-section of the wire target to that of a mass target. Stanton reported analytic solutions relating to sound scattering by cylinders of infinite and finite lengths[(16)]; however, in this work the end effects of the cylinders were neglected. In the present study, we have experimentally investigated the scattering cross-sections of wire targets and mass targets using a commercial US device. We propose the proper angle of the measurement plane to a wire target to adjust the effective size of the wire target to that of a mass target to enable the construction of an ultrasound calcification phantom using wire targets.

* Graduate School of Informatics, Kyoto University
Yoshida-honmachi, Sakyo-ku, Kyoto 606-8501, Japan
** Advanced Biomedical Engineering Research Unit, Kyoto University
Yoshida-honmachi, Sakyo-ku, Kyoto 606-8501, Japan
*** Graduate School of Medicine, Kyoto University
Yoshida-honmachi, Sakyo-ku, Kyoto 606-8501, Japan

2. Materials and Methods

2.1 Comparison of the Scattering Cross-Section of Wire Targets and Mass Targets Fig. 1 shows the schema for calcification depiction using CDDE. Since a calcification has a large acoustic impedance mismatch to soft tissue, creeping waves around the calcification surface, diffraction waves and multiple reflection waves in the calcification occur when a calcification exists in a scan line. When these waves occur at a calcification they cause the waveform of the ultrasound echo to change, and as a consequence the echo waveform of a scan line with a calcification is quite different from that without a calcification. This difference between the echo waveform of a scan lines with or without a calcification causes decorrelation of the echoes at and behind a calcification. Thus, the method depicts calcifications using cross-correlation between adjacent scan lines in an ultrasound B-mode image. CDDE has the potential to depict small calcifications that are undetectable in ultrasound B-mode images, and to approximate the performance of a US imager to that of an X-ray imager in terms of calcification depiction. In order to evaluate the performance of the method a calcification phantom with small targets that have inconspicuous echo intensities in comparison with their surroundings is needed. When a small mass target is employed its low echo intensity makes it difficult to confirm that it exists in a measurement plane. The employment of thin wire targets guarantees that the targets exist in all measurement planes. Therefore, we employed thin copper wires to investigate the performance of CDDE[13][14]. Calcification is a kind of mass target, and thus in evaluating the performance of CDDE in the depiction of calcification using US, the effective size of a wire target and a mass target should be similar. We thus investigated the scattering cross-sections of wire targets and mass targets experimentally.

The diameters of the copper wires and the sizes of the copper cylinders were all smaller than the beam width of the US device. This means that the echo intensity in a scan line at the target depth corresponds to the scattering cross-section of the target when the target is located close to the center of the scan line. As a consequence, we used the maximum echo intensity of a single scan line around the position of a wire target as the indicator of the scattering cross-section of the target, P.

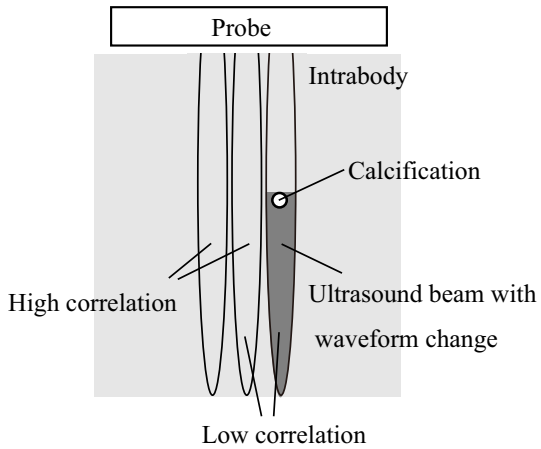

Fig. 1. Schema of the calcification depiction method using decorrelation of echoes caused by a calcification.

$$P \propto \max_{x,z \in S} I(x,z), \quad \cdots\cdots (1)$$

where x and z are respectively the lateral and vertical components of a pixel in a B-mode image, S is the region around a copper wire, and $I(x,z)$ is the echo intensity of a pixel in a B-mode image. Because the echo from a wire target has a specular echo component, the angle of the measurement plane to the wire is expected to strongly influence the echo intensity at the position of the wire. To acquire the proper angle of the measurement plane to adjust the scattering cross-section of a wire target to that of a mass target, we surveyed the variation in the scattering cross-sections of wire targets in response to variations in the angle of the measurement plane to the wires. Fig. 2 shows the scattering geometry of a copper wire.

The calculation of the scattering cross-section of a copper cylinder requires that the cylinder exists in the measurement plane. Therefore, we scanned the linear array probe to select the maximum echo intensity around the position of the cylinder.

2.2 Experimental Setup This study was mainly designed to depict calcifications that accompany breast cancers. We thus set the measurement depth at 1 to 3 cm. Since mammography can depict small calcifications of 0.2 and 0.1 mm in size[17][18], the depiction of small calcifications of the same sizes using CDDE is desirable. Therefore, we employed mass targets of 0.2 and 0.1 mm in size. The scattering cross-section of a wire

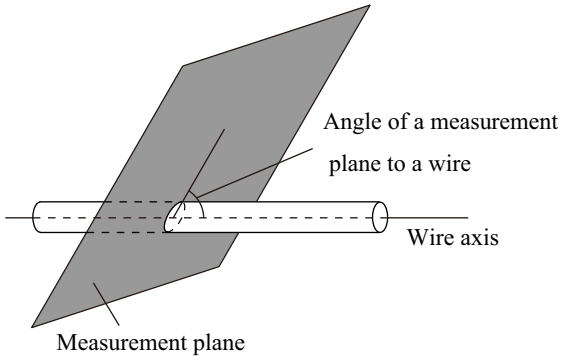

Fig. 2. Scattering geometry of a copper wire.

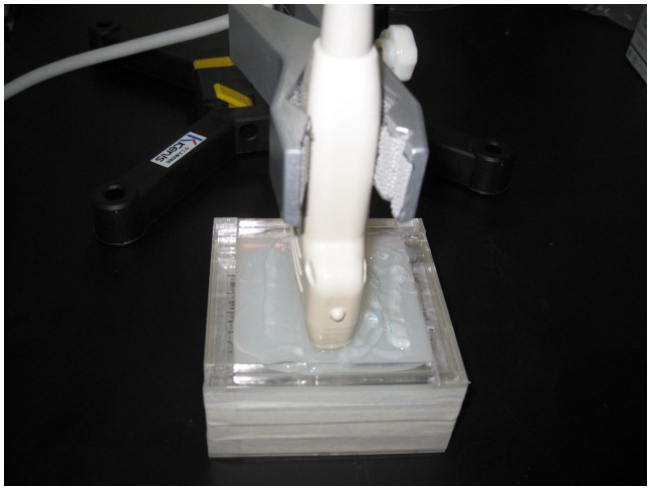

Fig. 3. Experimental apparatus for the evaluation of the effective size of wire targets.

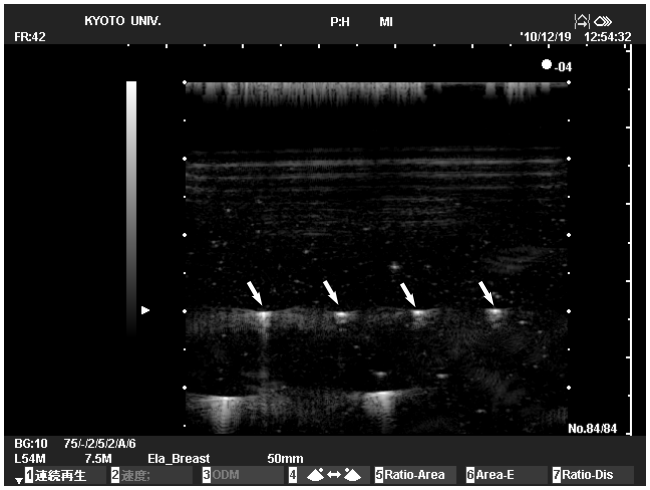

Fig. 4. B-mode image of a calcification phantom with four copper wires at a depth of 3 cm. The diameters of the copper wires are, from left to right, 0.2, 0.1, 0.05 and 0.03 mm.

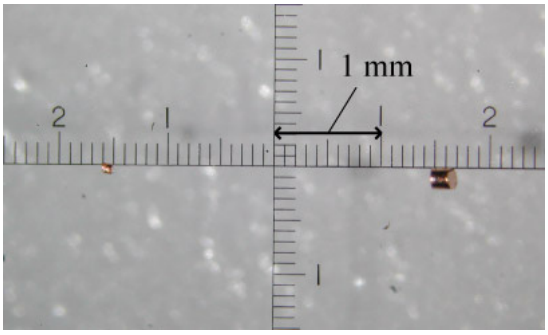

Fig. 5. Microscopic image of two copper cylinders of 0.1 and 0.2 mm in size located adjacent to a millimeter scale.

target is supposed to be larger than that of a mass target. For this reason we experimentally compared the scattering cross-sections of wire targets that were 0.2, 0.1, 0.05 and 0.03 mm in diameter and mass targets that were 0.2 and 0.1 mm in size. First, we prepared 4% agar gel block phantoms with wire targets embedded at depths of 1, 2 and 3 cm in three separate containers. Each phantom had four copper wires with diameters of 0.2, 0.1, 0.05 and 0.03 mm. Fig. 3 shows the experimental apparatus used in this study and Fig. 4 shows a B-mode image of a phantom with four wires. Next, we used copper cylinders that were 0.2 and 0.1 mm in size as mass targets, as shown in Fig. 5. The 0.2 mm copper cylinder was 0.2 mm in both diameter and length, and the 0.1 mm copper cylinder was 0.1 mm in both diameter and length. We then prepared 4% ager gel block phantoms with the copper cylinders embedded at depths of 1, 2 and 3 cm in three separate containers. Each phantom had five copper cylinders of 0.2 mm in size and five copper cylinders of 0.1 mm in size. Fig. 6 shows a B-mode image of a measurement plane with the two sizes of copper cylinders. To locate the copper cylinders at the target depth we first prepared an agar gel block that was 1 cm in thickness. We placed the cylinders on the surface of the block, and constructed

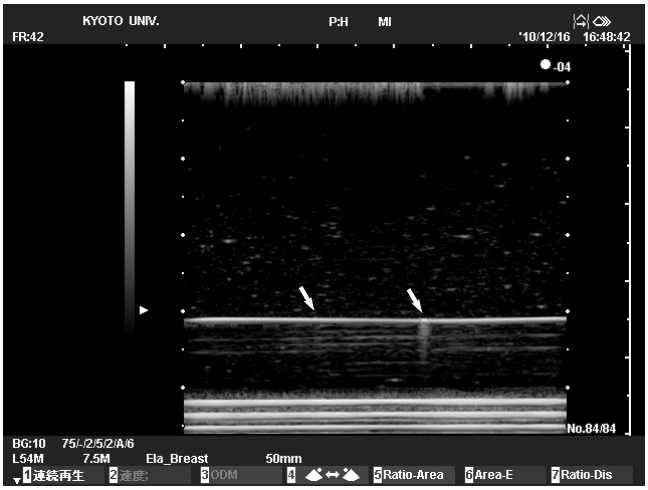

Fig. 6. B-mode image of a calcification phantom with two types of copper cylinders at a depth of 3 cm. The sizes of the copper cylinders are 0.1 (left) and 0.2 mm (right).

another gel block (1, 2 or 3 cm thick) on top of the gel block. This process produced a boundary at the depth of the cylinder targets. Experiments were conducted using a Hitachi EUB-8500 (Hitachi, Tokyo, Japan) US device with a 7.5 MHz linear array. In this study, we collected ten echo intensities for each type of the targets.

3. Results and Discussion

Fig. 7 shows the scattering cross-sections of the 0.2, 0.1, 0.05 and 0.03 mm diameter copper wires, and of the 0.2 and 0.1 mm copper cylinders at depths of 1, 2 and 3 cm, where each cross-section was normalized to the maximum scattering cross-section of a 0.2 mm diameter copper wire at the same depth. A small decrease in the angle of the measurement plane to a wire largely suppressed the scattering cross-section of the wire. This result means that the prime component of the echo from a wire target is the specular echo and indicates that this component is suppressed when the angle of the measurement plane is not perpendicular to the wire.

The 0.1 and 0.05 mm diameter wires had very similar scattering cross-sections at a depth of 3 cm. The scattering cross-section of a rigid and fixed cylinder of infinite length at the forward scattering direction in a far field was reported by Stanton[16].

$$P_{\text{wire}} \propto \left| \sum_{m=0}^{\infty} (-1)^m \varepsilon_m \frac{J_m'(ka)}{H_m^{(1)}'(ka)} \right|^2, \quad \cdots\cdots (2)$$

$$\varepsilon_m = \begin{cases} 1 & (m = 0) \\ 2 & (m \geq 1) \end{cases}, \quad \cdots\cdots (3)$$

where m is an integer, k is the wave number, a is the radius of the cylinder, $J_m'(x)$ is the derivative of the Bessel function of the first kind of order m, and $H_m'(x)$ is the derivative of the Hankel function of order m. This solution is derived from the well-known formulation for the scattering of sound by an infinitely long cylinder[19] in a cylindrical coordinate system with the condition of a plane wave incidence. This solution introduces the following assumptions. First, that there was no absorption, dispersion, or

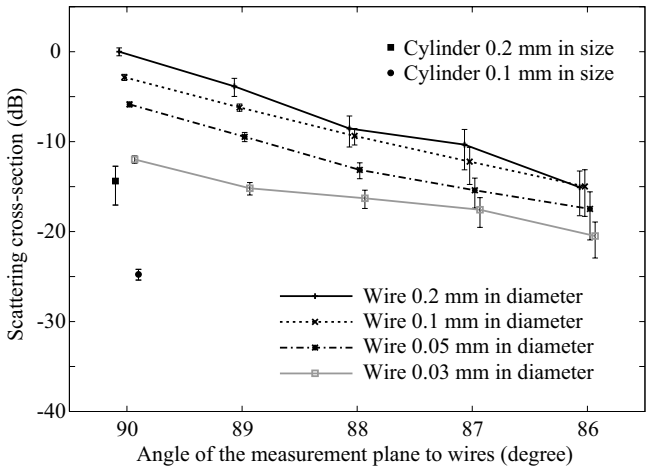

(a)

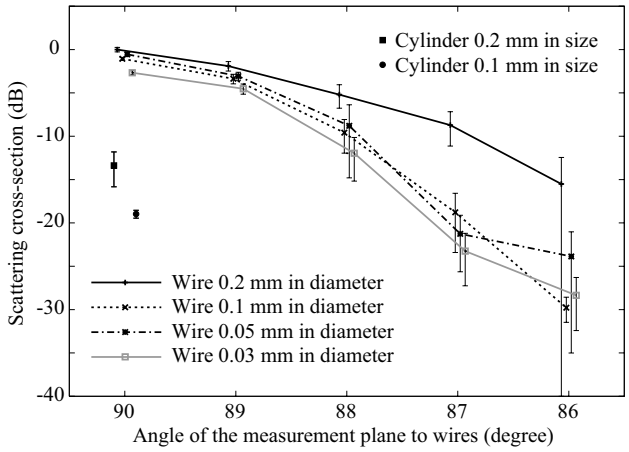

(b)

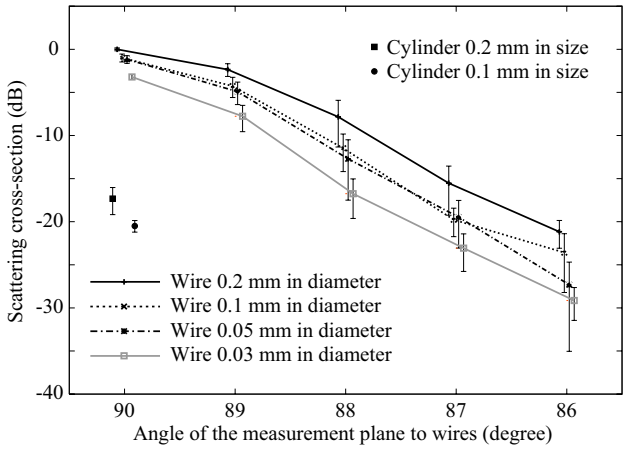

(c)

Fig. 7. Scattering cross-sections of four copper wires of diameters 0.2, 0.1, 0.05 and 0.03 mm and two copper cylinders 0.2 and 0.1 mm in size. Wires and cylinders are embedded at depths of (a) 1, (b) 2 and (c) 3 cm. The scattering cross-sections of the wires vary in response to the variations in the angle of the measurement plane to the wires. Each error bar shows a half of the standard deviation.

nonlinearities in the cylinder or surrounding medium. Second, that this solution does not support shear waves. In addition, that the end effect of a cylinder was not important. Applying this formula at the frequency of 7.5 MHz, the scattering cross-sections of the 0.1, 0.05 and 0.03 mm diameter wire targets are −5.27, −5.53, and −11.0 dB, respectively, where they are normalized to that of a 0.2 mm diameter wire target. When the angle of the measurement plane is 88 degrees or less the phase rotation of the echo from a wire occurs on an element surface. In this condition the signal received by an element is approximately equivalent to the sum of the two signals received at both ends of the element. Stanton[16] employed a point transmitter and a point receiver, and thus the experimental condition that uses a small angle of the measurement plane approaches the condition supposed by this author. As shown in Fig. 7 (c), when the angle of the measurement plane to the wires was 88 degrees the scattering cross-sections of the 0.1, 0.05 and 0.03 mm diameter copper wires were −3.65, −4.89 and −8.91 dB, respectively, where they were normalized to that of a 0.2 mm diameter copper wire at a depth of 3 cm. When the angle was 87 degrees the scattering cross-sections of the 0.1, 0.05 and 0.03 mm diameter wires at a depth of 3 cm were −4.25, −3.95, and −7.54 dB, respectively. Thus, in the theoretical study and in the experimental study, the scattering cross-sections of the wires 0.1 and 0.05 mm in diameter were very close. These results support the validity of the experimental study.

The scattering cross-sections of the 0.2 mm copper cylinders had a larger variance than that of the 0.1 mm cylinders. The scattering cross-section of a finite cylinder without the end effect was calculated as follows[16]:

$$P_{\mathrm{cln}} \propto L^2 \left(\frac{\sin(kL\cos\theta)}{kL\cos\theta} \right) \left| \sum_{m=0}^{\infty} (-1)^m \varepsilon_m \frac{J_m'(Ka)}{H_m^{(1)}'(Ka)} \right|^2, \quad \cdots\cdots (4)$$

where L is the length of a cylinder, θ is the angle between the incident direction of an ultrasound pulse and the cylinder axis, as shown in Fig. 8, and $K = k \sin\theta$. This solution was derived from the integration of the volume flow per unit length along the length of the cylinder[20] with the same assumptions at the solution of Eq. (2). Because this formula neglects the end effect of a cylinder, it cannot be applied when θ is smaller than 45 degrees due to the effect of the echo from the cylinder edges. Fig. 9 shows the variation in the scattering cross-sections of the 0.2 and 0.1 mm cylinders calculated by the formula, where each value of the scattering cross-section has been normalized to the maximum scattering cross-section of the 0.2 mm cylinder. This formulation

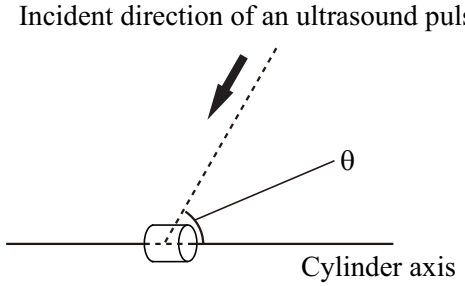

Fig. 8. Scattering geometry of a copper cylinder. θ denotes the angle between the incident direction of an ultrasound pulse and the cylinder axis.

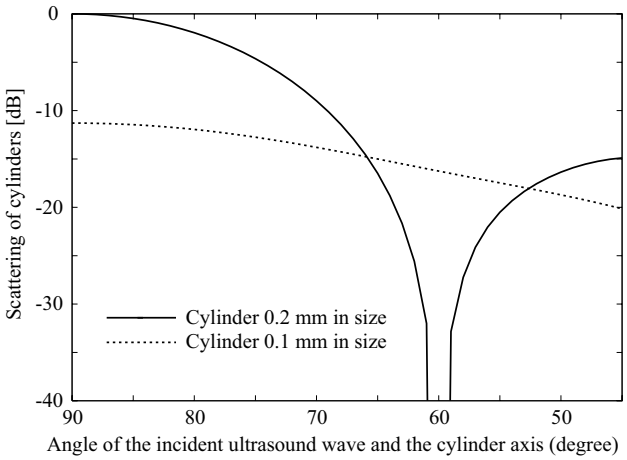

Fig. 9. Theoretical values of the scattering cross-sections of 0.2 and 0.1 mm cylinders in response to the angle of the incident ultrasound wave and the cylinder axis at a frequency of 7.5 MHz.

shows that at the frequency of 7.5 MHz the scattering cross-section of the 0.2 mm cylinder is severely suppressed when θ is close to 60 degrees. In contrast, the scattering cross-section of the 0.1 mm cylinder reduces gradually in response to a decrease in θ. These results indicate that the scattering cross-section of a 0.1 mm cylinder is less dependent on the direction of the cylinder axis, in agreement with the lower variance of a 0.1 mm copper cylinder investigated experimentally.

When the angle of the measurement plane to the wires was 90 degrees the scattering cross-sections of the wires was much larger than that of the cylinders. In contrast, a decrease in the angle of the measurement plane suppressed the scattering cross-sections of the wires to a less extent than that of the cylinders. Table 1 shows the angle of the measurement plane that was required to adjust the mean scattering cross-sections of wire targets to those of mass targets, where we utilized a logarithmic interpolation. The standard deviations of the scattering cross-sections of the 0.1 and 0.2 mm cylinders are listed in parentheses, where each was a linear value normalized to the standard deviation of the scattering cross-section of the wire after angle adjustment.

Subsequent to angle adjustment the variation in the scattering cross-section of a wire was different to that of a cylinder, as shown in parentheses in Table 1. This difference caused the disparity between the detectability of the cylinders and the wires. We thus investigated the cumulative values of the scattering cross-sections of the cylinders and a 0.1 mm diameter wire, where we assumed that the scattering cross-section of each type of target followed a normal distribution. Fig. 10 shows the detectability of 0.1 and 0.2 mm cylinders as compared with the detectability of a 0.1 mm diameter wire after angle adjustment. Each point in Fig. 10 indicates a cumulative value of the scattering cross-section of a wire and a cylinder at a given scattering cross-section value. This result showed that the detectability of a 0.2 mm cylinder approximates to that of a 0.1 mm diameter wire after angle adjustment; however, the estimation of the detectability of a 0.1 mm cylinder from the detectability of a wire requires compensation (Fig. 10). The employment of the angle adjustment with compensation, taking into consideration the variation in the scattering cross-section, will provide an experimental setup for the evaluation of an ultrasound calcification depiction method using wire targets.

Table 1. The angles of the measurement plane required to adjust the mean scattering cross-sections of 0.2, 0.1, 0.05 and 0.03 mm diameter copper wires to those of 0.2 and 0.1 mm copper cylinders, where the target depths are 1, 2 and 3 cm. The standard deviations of scattering cross-sections of the 0.1 and 0.2 mm cylinders are listed in parentheses, where each was a linear value normalized to the standard deviation of the scattering cross-section of the wire after angle adjustment.

		Cylinder of 0.2 mm in size	Cylinder of 0.1 mm in size
Depth of 1 cm	0.2 mm	86.2º (0.90)	
	0.1 mm	86.2º (0.90)	
	0.05 mm	87.5º (1.7)	
	0.03 mm	89.3º (3.3)	
Depth of 2 cm	0.2 mm	86.3º (0.56)	
	0.1 mm	87.6º (0.86)	87.0º (0.16)
	0.05 mm	87.6º (0.61)	87.2º (0.16)
	0.03 mm	87.9º (0.81)	87.4º (0.18)
Depth of 3 cm	0.2 mm	86.7º (0.70)	86.1º (0.41)
	0.1 mm	87.3º (0.89)	86.8º (0.38)
	0.05 mm	87.3º (0.58)	86.9º (0.26)
	0.03 mm	87.9º (0.72)	87.4º (0.33)

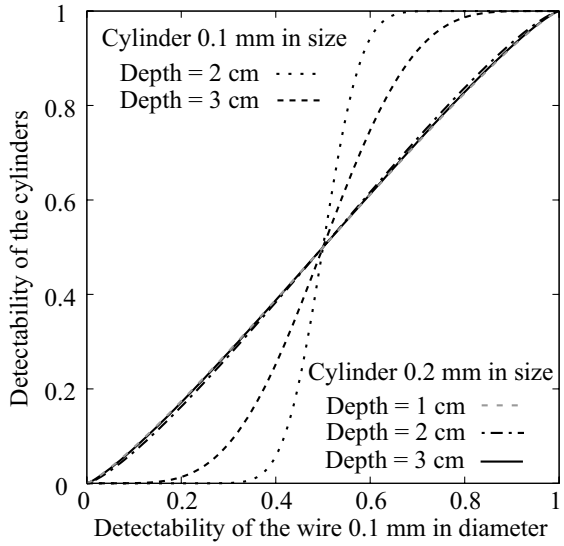

Fig. 10. Detectability of 0.1 and 0.2 mm cylinders as compared with the detectability of a 0.1 mm diameter wire after angle adjustment.

4. Conclusion

For the construction of an ultrasound calcification phantom using wires, we investigated the angle of the measurement plane to a wire as a method for adjusting the effective size of a wire target to that of a mass target. To acquire the proper angle of the measurement plane we compared the scattering cross-sections of 0.2, 0.1, 0.05 and 0.03 mm diameter copper wires and 0.2 and 0.1 mm copper cylinders at depths of 1, 2 and 3 cm. The experiments

were conducted using a commercial ultrasonographic device with a 7.5 MHz linear array probe. It was found that the scattering cross-section of a wire severely reduced as the angle of the measurement plane to the wire decreased. When the angles of the measurement planes to the wire were 87.6 and 87.0 degrees, the scattering cross-section of a 0.1 mm diameter copper wire was equivalent to those of 0.2 and 0.1 mm copper cylinders at a depth of 2 cm, respectively. Since the variation in the scattering cross-section of a 0.2 mm cylinder was similar to that of a 0.1 mm diameter wire after adjustment of the angle of the measurement plane, the detectability of a 0.2 mm cylinder approximated to that of a 0.1 mm diameter wire after angle adjustment; however, there was considerably less variation in the scattering cross-section of a 0.1 mm cylinder than in the scattering cross-section of a 0.1 mm diameter wire after angle adjustment, resulting in a necessity of compensation in order to estimate the detectability of a 0.1 mm cylinder from the detectability of a wire. This finding indicated that the employment of the proper angle of the measurement plane and appropriate compensation of detectability using the variation in the scattering cross-sections adjusted the effective size of a wire target to the size of a mass target, and consequently fulfilled the requirements for use as a calcification phantom. Future work will involve investigation of the performance of CDDE in calcification detection using the calcification phantom proposed in this study.

Acknowledgements

This work is partly supported by the Research and Development Committee Program of the Japan Society of Ultrasonics in Medicine and the Innovative Techno-Hub for Integrated Medical Bio-imaging Project of the Special Coordination Funds for Promoting Science and Technology from the Ministry of Education, Culture, Sports, Science and Technology (MEXT), Japan.

References

(1) H. Özdemir, M. K. Demir, O. Temizöz, H. Genchellac, and E. Unlu : "Phase inversion harmonic imaging improves assessment of renal calculi: a comparison with fundamental gray-scale sonography", J. Clin. Ultrasound, Vol.36, pp.16-19 (2008)

(2) K. A. B. Fowler, J. A. Locken, J. H. Duchesne, and M. R. Williamson : "US for detecting renal calculi with nonenhanced CT as a reference standard", Radiology, Vol.222, pp.109-113 (2002)

(3) P. M. Lamb, N. M. Perry, S. J. Vinnicombe, and C. A. Wells : "Correlation between ultrasound characteristics, mammographic findings and histological grade in patients with invasive ductal carcinoma of the breast", Clin. Radiol., Vol.55, pp.40-44 (2000)

(4) D. Jacob, J. C. Brombart, C. Muller, C. Lefèbvre, F. Massa, and A. Depoerck : "Analysis of the results of 137 subclinical breast lesions excisions. Value of ultrasonography in the early diagnosis of breast cancer", J. Gynecol. Obstet. Biol. Reprod., Vol.26, pp.27-31 (1997)

(5) S. J. Rosenthal, P. H. Jones, and L. H. Wetzel : "Phase inversion tissue harmonic sonographic imaging: a clinical utility study", AJR AM. J. Roentgenol., Vol.176, pp.1393-1398 (2001)

(6) K. T. Szopinski, A. M. Pajk, M. Wysocki, D. Amy, M. Szopinska, and W. Jakubowski : "Tissue harmonic imaging: utility in breast sonography", J. Ultrasound Med., Vol.22, pp.479-487 (2003)

(7) E. L. Rosen and M. S. Soo : "Tissue harmonic imaging sonography of breast lesions improved margin analysis, conspicuity, and image quality compared to conventional ultrasound", Clin. Imaging, Vol.25, pp.379-384 (2001)

(8) Y. Zhu and J. P. Weight : "Ultrasonic nondestructive evaluation of highly scattering materials using adaptive filtering and detection", IEEE Trans. Ultrason. Ferroelect. Freq. Contr., Vol.41, pp.26-33 (1994)

(9) N. Kamiyama, Y. Okamura, A. Kakee, and H. Hashimoto : "Investigation of ultrasound image processing to improve perceptibility of microcalcifications", J. Med. Ultrasonics, Vol.35, pp.97-105 (2008)

(10) H. M. Finn and R. S. Johnson : "Adaptive detection mode with threshold control as a function of spatially sampled clutter-level estimates", RCA Rev., Vol.29, pp.414-465 (1968)

(11) V. G. Hansen and H. R. Ward : "Detection performance of the cell averaging LOG/CFAR receiver", IEEE Trans. Aerosp. Electron. Syst., Vol.5, pp.648-652 (1972)

(12) H. Taki, T. Sakamoto, M. Yamakawa, T. Shiina, and T. Sato : "Small Calculus detection for medical acoustic imaging using cross-correlation between echo signals", Proc. IEEE Ultrason. Symp., pp.2398-2401 (2009)

(13) H. Taki, T. Sakamoto, M. Yamakawa, T. Shiina, and T. Sato : "Calculus Detection for Ultrasonography Using Decorrelation of Forward Scattered Wave", J. Med. Ultasonics, Vol.37, No.3, pp.129-135 (2010)

(14) H. Taki, T. Sakamoto, M. Yamakawa, T. Shiina, K. Nagae, and T. Sato : "Small Calcification Depiction in Ultrasound B-mode Image Using Decorrelation of Echoes Caused by Forward Scattered Wave", J. Med. Ultasonics, Vol.38, No.2, pp.73-80 (2011)

(15) H. Taki, T. Sakamoto, M. Yamakawa, T. Shiina, and T. Sato : "Indicator of Small Calcification Detection in Ultrasonography using Decorrelation of Forward Scattered Waves", Proc. International Conference on Computer, Electrical, and Systems Sciences, and Engineering, pp.175-179 (2010)

(16) T. K. Stanton : "Sound scattering by cylinders of finite length. I. Fluid cylinders", J. Acoust. Soc. Am., Vol.83, pp.55-63 (1988)

(17) R. H. Behrman, R. G. Zamenhof, and K. M. Blazo : "Evaluation of a commercial mammography image-enhancement system", J. Digital Imaging, Vol.2, No.3, pp.163-169 (1989)

(18) J. A. Manzano-Lizcano, C. Sánchez-Ávila, and L. Moyano-Pérez : "A microcalcification detection system for digital mammography using the contourlet transform", Proc. International Conference on Computational & Experimental Engineering & Science, pp.611-616 (2004)

(19) L. Rayleigh : Theory of Sound, Dover, New York (1945)

(20) E. Skudrzyk : The Foundations of Acoustics, Springer, New York (1971)

Hirofumi Taki (Member) received a M.D. degree from Kyoto University in 2000, a Ph.D. degree in informatics from Kyoto University in 2007, and is presently a research staff at Kyoto University. He has worked on the development of the spatial resolution and calcification detection ability in Ultrasonography. IEEE, Japan Society of Ultrasonics in Medicine, Acoustic Society of Japan, The Institute of Electronics, Information and Communication Engineers, Japan Society for Medical and Biological Engineering member.

Takuya Sakamoto (Member) received his B.E. degree from Kyoto University in 2000, and M.I. and Ph.D. degrees from the Graduate School of Informatics, Kyoto University in 2002 and 2005, respectively. He is an assistant professor in the Department of Communications and Computer Engineering, Graduate School of Informatics, Kyoto University. His current research interest is in ultra-wideband radar systems and ultrasonic signal processing. He is a member of the IEICE, the IEEJ and the IEEE.

Makoto Yamakawa (Member) was born in Fukui, Japan, on May 8, 1975. He received a Ph. D. degree in engineering from University of Tsukuba in 2002, and is presently an associate professor at Kyoto University. He has worked on tissue characterization using ultrasound. Japan Society of Ultrasonics in Medicine, The Institute of Electronics, Information and Communication Engineers member.

Tsuyoshi Shiina (Member) was graduated from the Electronic Engineering Department, the University of Tokyo, in 1982. He received the MS and PhD degrees in electronic engineering in 1984 and 1987, respectively, from the University of Tokyo. He also received Dr. of Medical Science in 2006, from University of Tsukuba. He has been a Professor of Graduate School of Systems and Information Engineering, the University of Tsukuba since 2001. He is presently a Professor of Graduate School of Medicine, Kyoto University. His current research interests include visualization technique of structural and functional bio-information, for example, ultrasonic elasticity imaging and brain function imaging. He was awarded Prizes for Science and Technology about Real-Time Tissue Elasticity Imaging System by Minister of Education, Culture, Sports, Science and Technology, 2010. He is Councilor of the Japan Society of Medical Electronics and Biological Engineering. He is also Executive Trustee of the Japan Society of Ultrasonics in Medicine (JSUM).

Toru Sato (Member) received his B.E., M.E., and Ph.D. degrees in electrical engineering from Kyoto University, Kyoto, Japan in 1976, 1978, and 1982, respectively. He is currently a Professor at Graduate School of Informatics, Kyoto University. His major research interests include system design and signal processing aspects of UWB radars and radar remote sensing of the atmosphere.